Tellus (1986), *38A*, 285–294

Nonlinear balance and gravity-inertial wave saturation in a simple atmospheric model

By T. WARN and R. MENARD, *Department of Meteorology, McGill University, 805 Sherbrooke Street West, Montreal, Quebec, Canada H3A 2K6*

(Manuscript received July 16; in final form October 23, 1985)

ABSTRACT

Numerical experiments with a highly truncated, forced-dissipative version of the shallow water equations suggest that for realistic atmospheric parameters, high-frequency inertial-gravity waves are almost always present in the solution, even in the limit of small Rossby numbers and long times. The waves are intermittent in character and appear to be generated naturally by the nonlinear interactions of the system. This behaviour is at variance with the notion that under normal atmospheric scaling, there is an attracting invariant manifold embedded in the full phase space which is completely free of fast oscillations (i.e., corresponding to "super quasi-geostrophic" motion). The high-frequency component leads to systematic differences between actual flow and high-order balanced states, suggesting that there is an inherent limitation to the amount of information about the divergent part of the flow that can be gleaned from the rotational motion. The information is expected to be a rapidly decreasing function of Rossby number.

1. Introduction

A disparity between the frequencies of the physical processes which contribute to the forcing of large-scale atmospheric motion and those of inertial-gravity waves leads to a slowly varying, nearly balanced (i.e., quasi-geostrophic) observed state. One possible consequence of this mismatch in time scales is that the observed flow is sufficiently constrained so as to require fewer degrees of freedom for its description than would otherwise be the case. More precisely, if the evolution is described in terms of a state vector moving in an appropriately defined phase space V, then the observed states might be expected to be confined to a lower dimensional surface or manifold, an observation which seems to have prompted Leith 1980) and Lorenz (1980) to introduce independently the "slow" or invariant manifold M. M is the set of balanced or quasi-geostrophic states which is thought to be of lower dimension than the full space (dimension N_{R}, where N_{R} is the number of rotational or slow modes of the system). M is thought to be invariant since "any state vector in M would continue to move in it," (Leith, 1980). In other words, any initially balanced state remains balanced at subsequent times. Lorenz (1980) terms the motion "superbalanced" since it is a generalization, supposedly accurate to all orders in Rossby number of earlier classical balancing, e.g., geostrophy, nonlinear balance equation (Charney, 1955).

The notion that the flow is restricted to a slow manifold seems self-consistent in the sense that the local Rossby number, defined as

$$\varepsilon_k = \frac{[E(k)k]^{1/2}k}{f},$$

where $E(k)$ is the energy spectrum, remains small at large wavenumbers due to the rapid decrease in spectral energy with scale in quasi-geostrophic turbulence (slope equal to -3 or even steeper; Kraichnan (1967), Charney (1971), Fornberg (1977) and Basdevant et al. (1981)). The a priori assumption of quasi-geostrophy is consistent with the a posteriori conclusion of a steep spectral slope. One is left with the impression that the motion is superbalanced at all orders on all scales, and that the observed transition from quasi-geostrophy at large scales to ageostrophic flow at short scales is a manifestation of neglected physical processes (e.g. ragged topography, convection, etc.). This picture is somewhat conterintuitive, at least to the authors, and it seems worthwhile to re-examine the arguments underlying the notion of the slow manifold. Of interest in this regard is the work of Sadourny (1975), Errico (1984), and Warn (1986) which indicates that truncated inviscid systems inevitably become unbalanced due to a gradual transfer of energy into the high-frequency inertial-gravity waves. In other words, the spectrum of quasi-geostrophic motion appears to be unstable in the statistical mechanical limit. If this instability survives in forced-dissipative flows, it could contribute to the shallowness of observed spectra at short scales. Alternately the instability might be suppressed by dissipation. Earlier work by Errico (1982) and that of Warn (1986) as well as the numerical results presented below suggest the former alternative when the dissipation is small. In any event, dissipation seems necessary for the existence of the slow manifold.

A number of algorithms based on the (implicit) assumption of small Rossby number and slow timescales have been proposed for constructing a sequence of manifolds $U^{(n)}$. Here we restrict ourselves to the one proposed by Lorenz (1980). The method is closely related to the method of normal mode initialization (Leith, 1980; Machenhauer, 1977) or the bounded derivative method (Kreiss, 1979); see also Kopell (1985), Warn (1986) and Vautard and Legras (1985) for discussions and further references. The assumption that the sequence, $U^{(n)}$, converges to an invariant manifold then leads to the "slave" relation

$$G = \varepsilon U(R, \varepsilon), \tag{1}$$

between the fast and the slow modes, valid for small enough Rossby numbers. (1) serves to define M. In this expression, G and R are vectors whose components are the amplitudes of the fast (gravity-inertial) and slow modes (Rossby or rotational) used in the normal mode representation of the dependent variables (Leith, 1980). It is diagnostic and can be identified with the (spectral) versions of the classical balance and ω-equations extended to infinite order in Rossby number. It can also be used to eliminate the G's from the equations governing the slow modes thereby providing a generalization of the usual quasi-geostrophic system supposedly accurate to all orders in Rossby number. The existence of a relation (1) would imply that long-time trajectories or states can be reconstructed from a knowledge of the rotational modes alone. The notion of an invariant manifold also plays a prominent role in modern initialization procedures wherein the R's and G's obtained from observations of the atmosphere are modified so as to lie on the manifold in the hope of preventing the artificial excitation of fast modes ("sloshing") due to observational or model error. It should be emphasized in this regard that the manifold must be global and attracting if it is to be useful in applications and that none of these properties has actually been proven for realistic scaling. (1) should also hold over a finite range of the R's, local manifolds known only to exist in the neighborhood of fixed points or "manifolds" involving Cantor structure are not of interest in the present context. The manifold must also be distinguished from the attractor, which is assumed to be embedded in it (Lorenz, 1980).

As discussed in Section 3, numerical calculations using the highly truncated shallow water system introduced by Lorenz (1980) indicate that non-trivial trajectories will almost always contain a high-frequency component (high-frequency oscillations have also been observed in another context by Errico (1982). Since the sequence $U^{(n)}$ is constructed assuming slow motion, it seems unlikely that it can converge to an attracting invariant manifold. The central issue consequently revolves around the existence of a slow manifold, which is uncertain unless other arguments can be found. One possibility might be to employ invariant manifold theorems (Carr, 1981; Guckenheimer and Holmes, 1983). There are however certain difficulties. The theory guarantees the existence of a manifold of the form (1) provided the *real parts* of the eigenvalues of the linear system satisfy certain constraints (e.g., a separation into fast and slow *attenuation* rates, see Carr, 1981). By contrast, the slow manifold definition depends on the properties of the imaginary part of the spectrum (i.e., the separation between fast and slow frequencies). It would appear that the theory can be used to establish the existence of the slow manifold only if the real and imaginary parts both satisfy the appropriate conditions. More specifically, the theory has been employed successfully only when there is differential damping in the sense that the attenuation rates of the inertial-gravity waves are significantly larger than those of the rotational modes. In the shallow water system used here, existence has been established only when the mass diffusion is relatively large and the Prandtl number, defined as the ratio of the viscosity and diffusion coefficients, approaches zero (Kopell, 1985). It is our view that this region of parameter space is of limited meteorological interest. A more relevant limit, and the one considered here, obtains when the damping is no larger than the order of the Rossby number, is preferably much smaller, and is of the same order for both the fast and slow modes (Prandtl number order one). It seems unlikely that invariant manifold theory can be applied in this case.

To summarize, the numerical experiments presented in the following sections suggest that under reasonable atmospheric scaling attracting invariant slow manifolds will not usually exist since almost every solution to the equations of motion involves some level of inertial-gravity wave generation when the dissipation is sufficiently small. This is also supported by the work of Errico (1982). An *invariant manifold* can be shown to exist for holomorphic systems without resonant eigenvalues (Vautard and Legras, 1985), however such systems are quite special since they are topologically equivalent to linear systems (Arnold, 1983, p. 188) and don't admit complex trajectories.

Given the demonstrated utility of balancing procedures it may seem surprising to conclude that the true solution almost never reaches a state of balance. In retrospect, however, this is not unexpected since the balance schemes are essentially expansions in Rossby number of a singular perturbation problem suggesting that an asymptotic (as opposed to an exact) representation is obtained (Kopell, 1985). As there are inherent limitations to the accuracy of such schemes, it is argued that these series can probably only be used to define balanced motion in terms of a "fuzzy" slow subset in phase space, the "fuzziness" being a consequence of ever present fast oscillations.

2. Model details

We shall employ the forced-dissipative, low-order, shallow water system described by Lorenz (1980). The flow is doubly periodic over a square with sides L in the horizontal, rotating, and driven by sources and sinks of mass. The effects of mass diffusion, viscosity, and topography are also included. Scaled versions of the dependent variables χ, the velocity potential, ψ, the stream function, z, the free surface height, as well as the forcing, F, and topography, h, are expanded in trigonometric series of the form

$$\chi = 2L^2 f \sum x_i \phi_i,$$

etc., where f is the rotation rate and

$$\phi_i = \cos(\boldsymbol{a}_i \cdot \boldsymbol{r}/L).$$

Only three scales are retained for which the dimensionless wavevectors satisfy

$$\boldsymbol{a}_1 + \boldsymbol{a}_2 + \boldsymbol{a}_3 = 0.$$

Substitution into the shallow water equations then leads to (Lorenz, 1980)

$$a_i \frac{\mathrm{d}x_i}{\mathrm{d}t} = a_i b_i x_j x_k - c(a_i - a_k) x_j y_k + c(a_i - a_j) y_j x_k - 2c^2 y_j y_k - v_0 a_i^2 x_i + a_i y_i - a_i z_i, \tag{2}$$

$$a_i \frac{\mathrm{d}y_i}{\mathrm{d}t} = -a_k b_k x_j y_k - a_j b_j y_j x_k + c(a_k - a_j) y_j y_k - a_i x_i - v_0 a_i^2 y_i, \tag{3}$$

$$\frac{\mathrm{d}z_i}{\mathrm{d}t} = -b_k x_j (z_k - h_k) - b_j (z_j - h_j) x_k + c y_j (z_k - h_k) - c(z_j - h_j) y_k + g_0 a_i x_i - k_0 a_i z_i + F_i. \tag{4}$$

v_0 and k_0 are scaled versions of the viscosity and diffusion and

$$a_i = \boldsymbol{a}_i \cdot \boldsymbol{a}_i,$$

$$b_i = \boldsymbol{a}_j \cdot \boldsymbol{a}_k,$$

$$c = \boldsymbol{a}_j \times \boldsymbol{a}_k \cdot \boldsymbol{k}.$$

For further details see Lorenz (1980). Eqs. (2)–(4) hold for cyclic permutations (i, j, k) of 1,2,3. The parameters are chosen according to Lorenz so as to conform with the atmosphere in temperate latitudes. Thus we take $\boldsymbol{a}_1$ to point northward, implying that the variables with subscript 1 represent a zonally uniform flow. The topography and forcing are also taken to be zonal, i.e., $h_2 = h_3 = F_2 = F_3 = 0$, while the scales are chosen so that $a_1 = a_2 = 1$ and $a_3 = 3$, whence $c^2 = \frac{1}{4}$. The remaining parameters are $f^{-1} = 3$ h, which corresponds to one dimensionless time unit, $h_1 = -1$, $g_0 = 8$, $v_0 = k_0 = \frac{1}{48}$, and F_1, which will be treated as a bifurcation parameter.

In the absence of forcing and topography, the linearized system has a damped rotational mode with eigenvalue $\lambda_i^R = -a_i v_0$, and two damped inertial-gravity modes with eigenvalues

$$\lambda_i^G = -a_i v_0 \pm i(1 + a_i g_0)^{1/2},$$

associated with each scale. The imaginary parts correspond to dimensionless (dimensional) gravity-inertial wave periods of ≈ 2.1 and 1.3 units (6.3 and 3.8 h). The dissipation timescales associated with these modes are 16 and 48 units (6 and 2 days) respectively. Note that the lower frequency is subject to the least damping. The numerical results of the next section indicate that except for steady flows, a high-frequency component corresponding to this mode is almost always present in the solution to some degree.

In the absence of x-dependent forcing and topography, eqs. (2)–(4) have a steady, zonally symmetric or Hadley solution with $\bar{x}_i, \bar{y}_i, \bar{z}_i = 0$, $i = 2, 3$, and

$$\bar{x}_1 = -\frac{F_1}{|\lambda_1^G|^2},$$

$$\bar{y}_1 = \frac{F_1}{v_0|\lambda_1^G|^2},$$

$$\bar{z}_1 = \frac{(1 + v_0^2)F_1}{v_0|\lambda_1^G|^2}.$$

Certain aspects of the stability of this solution have been discussed by Gent and McWilliams (1982) while the stability of the Hadley and other equilibria have been treated in detail by Vautard and Legras (1985) from which Fig. 1 has been adapted. The figure gives the equilibrium value of $\bar{x}_3^{1/3}$ as F_1 varies. The Hadley solution lies on the horizontal axis. As indicated, the solution is stable (solid line) for small enough forcing. As F_1 passes through F_p (≈ 0.016), the Hadley solution is destabilized via a supercritical pitchfork bifurcation as an eigenvalue passes through zero into the positive half-plane and two new wavy equilibria appear ($\bar{x}_2$, $\bar{y}_2$, etc., non-vanishing). As F is increased further these new equilibria are destabilized via a Hopf bifurcation (Arnold, 1983; Guckenheimer and Holmes, 1983) of the rotational modes at F_{H2} (≈ 0.05, where a pair of low-frequency, complex conjugate eigenvalues cross the real axis). Both of these are quasi-geostrophic bifurcations in the sense that they also occur in the underlying quasi-geostrophic system (Lorenz, 1980; eq. (43)). At $F_1 = F_{H1}$ (≈ 0.0774), the (unstable) Hadley solution undergoes a *high-frequency* Hopf bifurcation as the lowest frequency gravity-inertial wave (dimensionless period ≈ 2.12) becomes unstable. This bifurcation has no counterpart in the quasigeostrophic system. It was originally thought that this instability might play a significant role in the generation of high-frequency inertial-gravity waves discussed above. The numerical results of the next section indicate otherwise since high-frequency oscillations are observed in the solution on either side of F_{H1}.

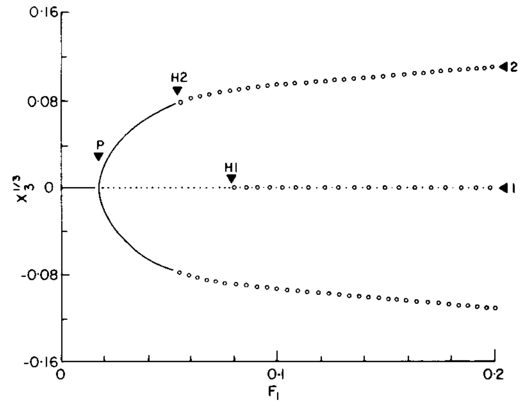

Fig. 1. Bifurcation diagram of the Hadley solution projected onto $\bar{x}_3^{1/3}$ (after Vautard and Legras, 1985) for the parameters given in the text. The Hadley solution is located on the horizontal axis. The solid line represents a stable solution while the dots and open circles indicate a single or complex conjugate pair of unstable eigenvalues respectively. In combination, both types are implied to exist, thus above H_1, the unstable manifold of the Hadley solution is three-dimensional.

Numerical integrations indicate that the trajectories tend to one of the stable fixed points for $F_1 \leqslant F_{H2}$, while in the range (F_{H2}, 0.7), they are either chaotic or periodic. Above $F_1 \sim 0.7$, the solution blows up.

Balanced states are defined in terms of a sequence of manifolds $U^{(n)}$ defined by the Lorenz algorithm, i.e., we introduce

$$G = \begin{bmatrix} x_1 \\ x_2 \\ x_3 \\ y_1 - z_1 \\ y_2 - z_2 \\ y_3 - z_3 \end{bmatrix},$$

and require

$$\frac{d^n G}{dt^n} = F^{(n)}(R, G),$$
$$= 0, \qquad (5)$$

where $R_i = y_i$. $F^{(n)}$ is found by repeated use of eqs. (2)–(4) and their derivatives with respect to t. For each n, N_G algebraic relations are defined, where N_G is the total number of gravity-inertial modes. When $n = 0$, the geostrophic limit $y_i = z_i$ and $x_i = 0$ is recovered and the manifold corresponds to $G = 0$. For higher orders, an infinite sequence of manifolds of the form (1) is obtained provided the Jacobian matrix, $\partial F^{(n)}/\partial G$, is nonsingular for each n. In the next section sequences of balanced states (up to order 40) are constructed by solving (5) iteratively using Lorenz's scheme and the degree of "imbalance", defined by $G - U^{(n)}(R)$ where G and R are obtained from long-time numerical integrations of eqs. (2)–(4), is examined for various values of F_1.

3. The numerical procedures and results

Eqs. (2)–(4) were integrated up to $t = 3{,}000$ (375 days) using a double precision (~16 digits), 8th order version of the Taylor series time-stepping scheme used by Lorenz (1980) with a timestep of $\frac{1}{24}$ dimensionless units. As high precision was required, a number of comparisons with runs using various combinations of precision and timestep (i.e., double versus quadruple precision, timesteps $\frac{1}{24}$ versus $\frac{1}{12}$) have been made. Except where indicated and aside from differences due to sensitivity to initial conditions when the attractor is strange, the results below are insensitive to these choices. Three runs with $F_1 = 0.07$, 0.1 and 0.2 were performed with initial conditions $x_i = y_i = z_i = 0.1$. The values for F_1 were chosen so as to allow the effects of the gravity-inertial bifurcation F_{H1} to be examined. The first run consequently gives an indication of the behaviour in the absence of the gravity-inertial wave instability. Examination of the long-time behaviour of the solutions indicates that the attractor set is strange for the first two runs and periodic for $F_1 = 0.2$ (Fig. 2).

The initial conditions, being unbalanced, lead to significant gravity-inertial wave excitation during the early stages (Fig. 3 for $F_1 = 0.07$, see also

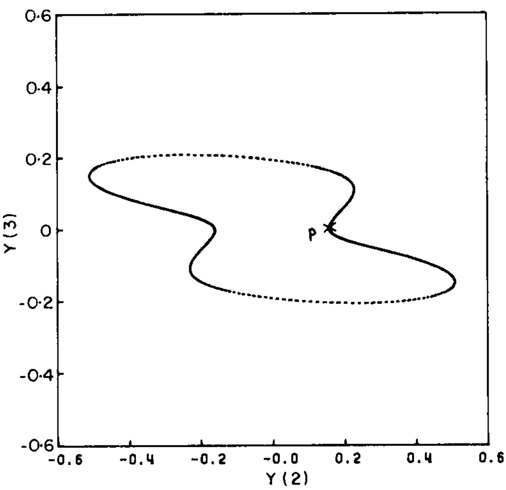

Fig. 2. Projection of the phase trajectory for $F_1 = 0.2$, onto the y_2–y_3 plane. The parameters are given in the text. The attractor seems periodic with a period of about 9 days. The sequence of balance residuals was calculated at P (see Section 3).

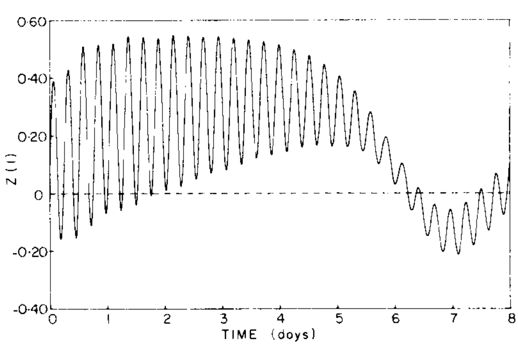

Fig. 3. Initial relaxation of gravity-inertial waves as shown by the time series of $z_1 \cdot F_1 = 0.1$.

Lorenz (1980), Fig. 3). The oscillations gradually decay due to the action of viscosity and diffusion and after about 15 days are no longer easily discernible. The behaviour at later times was examined by first calculating balanced states up to order 40 in both double and quadruple precision every 10 days and then constructing the "unbalanced" residual of the signal by subtracting the nth order balanced states from the full numerical solution, i.e., from $G - U^{(n)}(R)$. The residual, $x_1 - x_1^{(20)}$, is shown in Figs. 4–6 (actually the maximum imbalance over a six hour interval is shown, see below) for each run. It decays exponentially during the early stages at a rate consistent with the weakest gravity-inertial wave attenuation rate (dashed line on figures). On longer timescales, the imbalance saturates at a relatively low level being smallest when the forcing is small. An example of the fine structure of the imbalance is shown in Fig. 7 for F = 0.07. In this figure, the residual $x_1 - x_1^{(20)}$ is plotted every $\frac{1}{2}$ h for 12 h beginning at day 360.

The signal is nearly monochromatic and is easily identified with the lowest frequency inertial-gravity wave. Note that in this example, the amplitude of the high-frequency component is at least 13 orders of magnitude smaller than the main signal. The fine structure has also been examined for different times and different values of F_1. In each case the imbalance was a nearly monochromatic inertial-gravity wave with a period slightly greater than 2 dimensionless units (≈6 h). In fact in Figs. 4–6, the quantity actually plotted is the amplitude of the gravity-inertial wave extracted from a fine structure calculation performed every 10 days. Note that the overall saturation level indicated in these figures increases by 8 or 9 orders of magnitude in response to a moderate increase in the forcing (Rossby number) by about a factor of three, suggesting a transcendental as opposed to algebraic dependence of the gravity-inertial wave amplitude. After saturation, the behaviour is intermittent and can vary over several orders of magnitude. As mentioned above, the calculations have been checked in a number of ways (double vs single precision, smaller timesteps, using the residual from higher order balancing, etc.). These tests as well as the

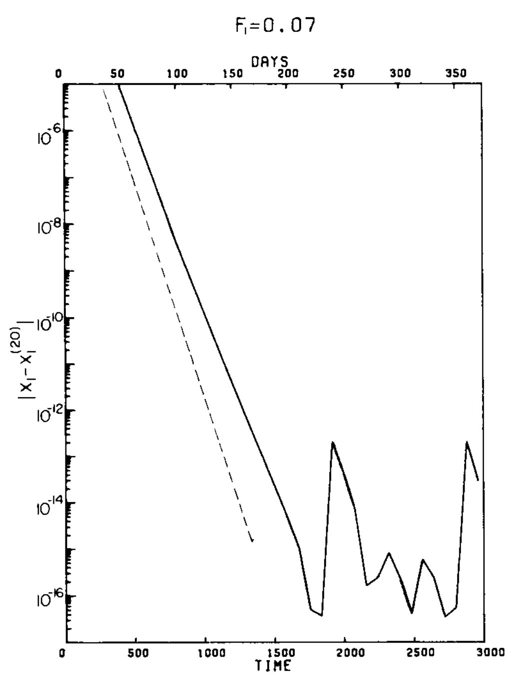

Fig. 4. Long time macroscale "imbalance" for $F_1 = 0.07$ as indicated by $|x_1 - x_1^{(20)}|$ calculated every 10 days. x_1 is obtained from integrations of eqs. (2)–(4) while $x_1^{(20)}$ is obtained from the 20th order balance scheme and y_i, $F_1 = 0.07$.

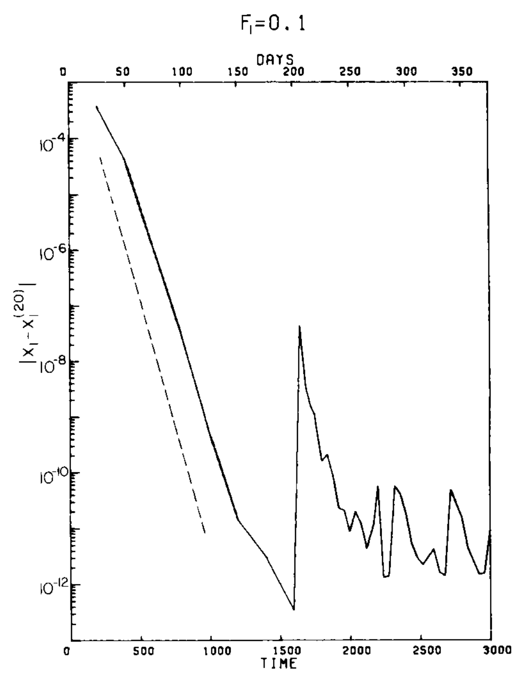

Fig. 5. Same as Fig. 4. except that $F_1 = 0.1$.

purity of the residual signal tend to support the accuracy of the calculations. Finally, a sequence of residual gravity-inertial wave amplitudes was calculated $F_1 = 0.02$ each time the trajectory passed through point P on Fig. 2. These were equal to three or more significant figures indicating that the residual is also periodic. The apparent aperiodicity indicated in Fig. 6 is an artifice of the sampling procedure.

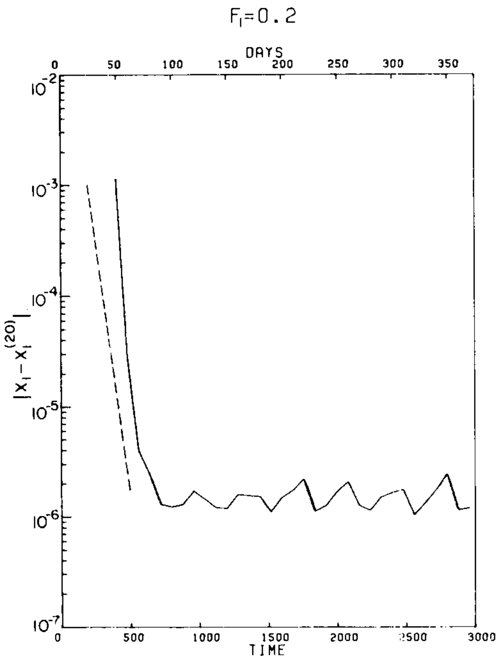

Fig. 6. Same as Fig. 4 except that $F_1 = 0.2$. Higher resolution in time indicates that the signal is actually periodic. The irregularity is due to the sampling interval.

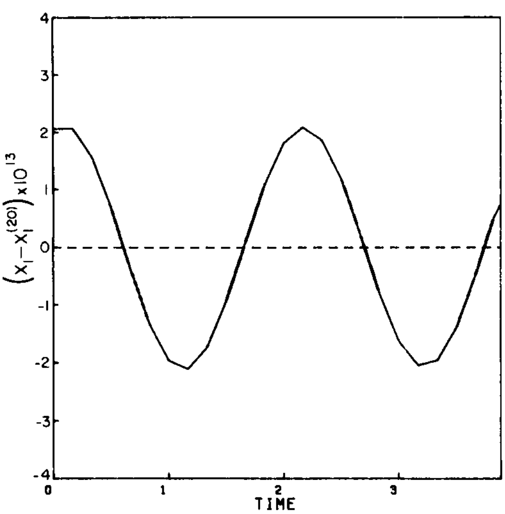

Fig. 7. As in Fig. 4 except for every $\frac{1}{2}$ h beginning at day 360.

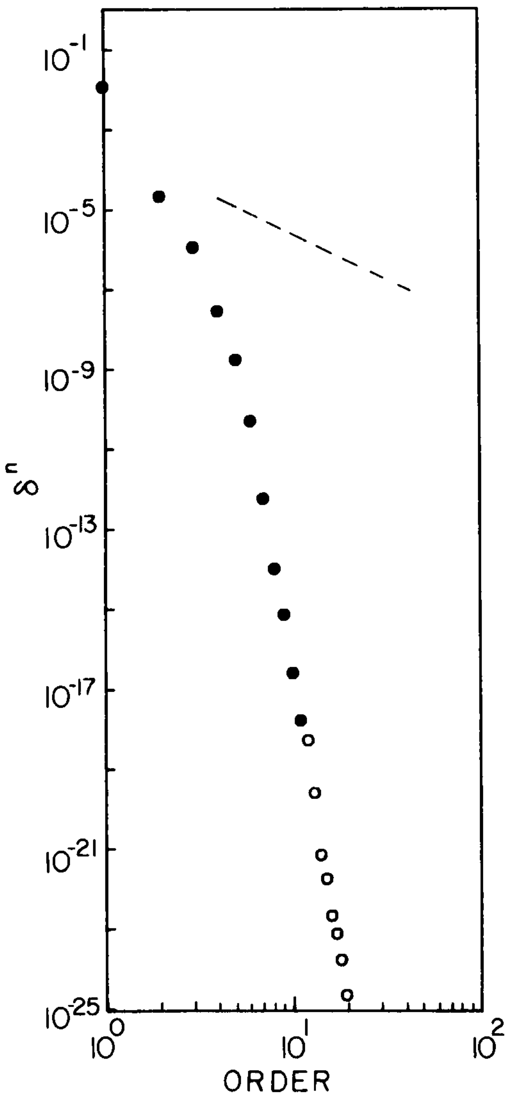

Fig. 8. $\delta^n = ||G^{(n)} - G^{(n+1)}||$ versus n. $F_1 = 0.1$ Dimensional time equals 200 days. The open circles indicate that a comparison of double and quadruple balance calculations differ in the first or second significant figure.

The behaviour of the sequence of manifolds up to $n = 40$ also been examined in a number of cases. Three different behaviours were observed.

(a) The balance condition was solvable at each order and the sequence $\delta^{(n)} = \|U^{(n)} - U^{(n+1)}\|$, where the Euclidean norm is implied, appeared to converge (e.g., the example shown in Fig. 8 converged to machine precision). Note that a slope exceeding -1 implies convergence. Despite the apparent convergence, the balanced flow differed systematically from the actual flow due to the presence of the residual inertial-gravity waves. The time series of the residual imbalance for each n was also examined and found to be nearly monochromatic and independent of n for n large enough. Alternately

(b) the balance sequence was solvable at each order although the sequence appeared to diverge, or at the very least, exhibited a marked deceleration in the rate of convergence. Specifically, there was a

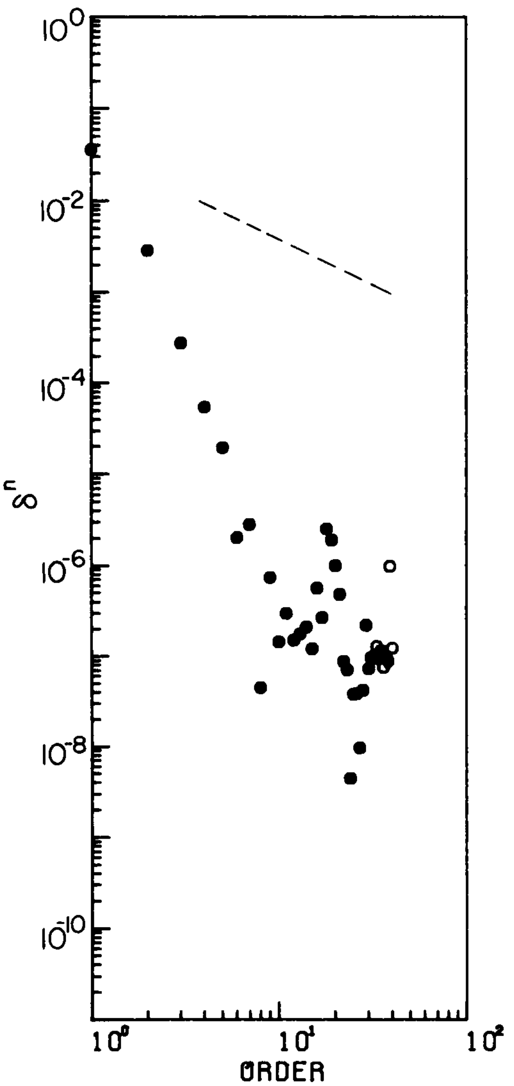

Fig. 9. As in 8 except that dimensional time equals 206 days.

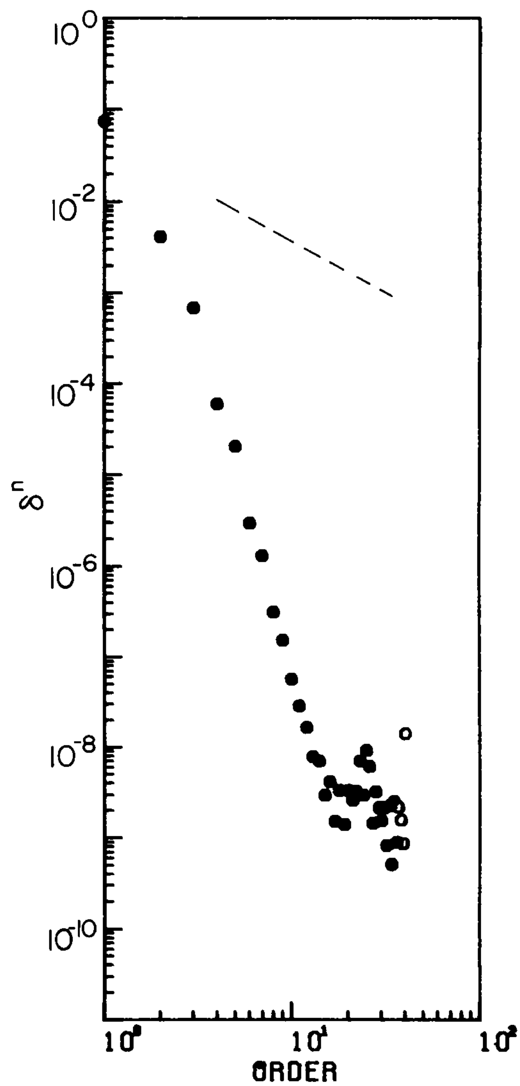

Fig. 10. As in 8 except $F_1 = 0.2$ and the dimensionless time equals 260 days.

suggestion that $\delta^{(n)}$ did not vanish as $n \to \infty$ (Figs. 9 and 10). Note that as n approached 40, the double versus quadruple calculations indicated some loss of precision (see figure caption). For $n \sim 30$ or less, the calculations agreed to many significant figures. The example shown in Fig. 10 was unique in the sense that the saturation level of $\delta^{(n)}$ was of the same order as the gravity inertial-wave residual indicating that the amplitude of the residual depends somewhat on n. Finally

(c) the iterative scheme used to obtain the balance at order n did not converge and no sequence of manifolds could be constructed. This behaviour was observed only for relatively large forcing. It was not observed for the runs presented here.

4. Discussion and conclusions

The above results seem to mitigate against the existence of a slow manifold, or at the very least, they indicate that if it exists, it is unstable, since, except for steady flows, the trajectories seem to possess a gravity-inertial wave component which persists for all time. If this is indeed the case, it becomes necessary to reconsider the definition of balanced flow for the truncated model under consideration. Since nonsteady solutions appear to involve some level of inertial-gravity wave activity, it seems reasonable to classify as balanced those regions of phase space involving a level of gravity wave activity consistent with that which would be generated naturally. The sequence of manifolds, $U^{(n)}$, can be regarded as an asymptotic sequence for the G's which can be used to define an open, somewhat "fuzzy" balanced set, B, which has the same dimension as the underlying space (Fig. 11). The vagueness in the definition of B is a consequence of the well-known fact that asymptotic series involve inherent limitations to their accuracy (Bender and Orszag, 1978, ch. 3).

It would be of interest to determine the degree of uncertainty in the nth order manifold or equivalently, to estimate the order of the amplitude of the inertial-gravity waves from the rotational modes since it could be of relevance for the initialization problem. The "fuzziness" could be of some advantage since the modifications required of the data to ensure balance might be substantially weakened allowing balanced initial states to more faithfully represent the initial data (i.e., the data point D of Fig. 11 could be modified to A_2 rather than A_1 and still be regarded as balanced). For small forcing (Rossby numbers) the differences between A_1 and A_2 will be slight since the high frequency component is small. For larger values, the difference could be significant, particularly given the rapid increase in amplitude as a function of the forcing. Many asymptotic sequences exhibit a characteristic behaviour wherein, $\delta^{(n)} = \| U^{(n)} - U^{(n+1)} \|$, first decreases and then increases as a function of n, with the optimal estimate given by $U^{(m)}$, where m is chosen so that $\delta^{(m)}$ is a minimum (Bender and Orszag, 1978). The error or "fuzziness" is then estimated by $\delta^{(m)}$. The balance sequences of Section 3 do not seem to have this property. For small enough forcing, $\delta^{(n)}$ was observed either to decrease monotonically to zero or to first decrease and then saturate for n large enough. When $\delta^{(n)}$ saturated, it usually did so at a level which was somewhat lower than the observed gravity wave amplitude. To date we have been unable to discover a simple means of estimating the level of gravity wave activity from instantaneous

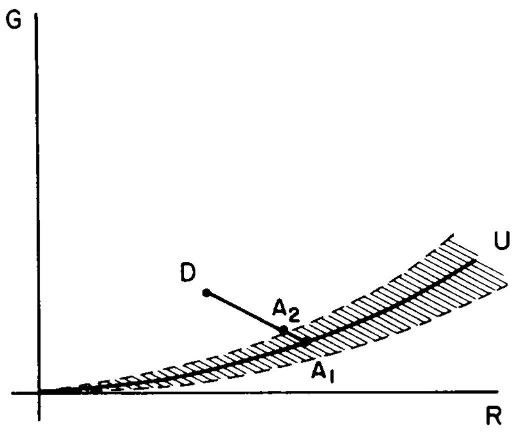

Fig. 11. The "fuzzy" balance set. If the trajectories of a model were confined to an invariant manifold U, then the model could be initialized by modifying the data D to produce initial conditions A_1 on the manifold. Since the model trajectories inevitably involve inertial-gravity waves, the actual trajectories are only constrained to lie somewhere in the hatched region, defined as that region of phase space with inertial-gravity waves at their saturation level. A_2 is consequently an equally viable initial condition and is closer to the observed initial state.

state of the rotational modes. Perhaps a statistical approach is required.

5. Acknowledgements

Part of this work was done when the first author was a visitor at the Laboratoire de Meteorologie Dynamique, Paris. Fruitful discussions with B. Legras, R. Vautard, R. Sadourny, and O. Talagrand are gratefully acknowledged. This research was supported in part by grants from NSERC and AES. The second author received support from FCAC.

REFERENCES

Arnold, V. I. 1983. *Geometrical methods in the theory of ordinary differential equations*. Springer. 334 pp.

Basdevant, C., Legras, B., Sadourny, R. and Beland, M. 1981. A study of barotropic model flows: Intermittency, waves and predictability. *J. Atmos. Sci. 38*, 2305–2306.

Bender, C. and Orszag, S. 1978. *Advanced mathematical methods for scientists and engineers*. McGraw-Hill. 593 pp.

Carr, J. 1981. *Applications of center manifold theory*. Springer, Berlin. 142 pp.

Charney, J. 1971. Geostrophic turbulence. *J. Atmos. Sci. 28*, 1087–1095.

Charney, J. 1955. The use of the primitive equations of motion in numerical weather prediction. *Tellus 7*, 22–26.

Errico, R. 1982. Normal mode initialization and the generation of gravity waves by quasi-geostrophic forcing. *J. Atmos. Sci. 39*, 573–586.

Errico, R. 1984. The statistical equilibrium solution of a primitive equations model. *Tellus 36A*, 42–51.

Fornberg, B. 1977. A numerical study of 2-D turbulence. *J. Comp. Phys. 25*, 1–31.

Gent, P. and McWilliams, J. 1982. Intermediate Model Solutions to the Lorenz Equations: Strange Attractors and Other Phenomena. *J. Atmos. Sci. 39*, 3–13.

Guckenheimer, J. and Holmes, P. 1983. *Nonlinear oscillations, dynamical systems, and bifurcations of vector fields*. Springer, Berlin. 453 pp.

Kopell, N. 1985. Invariant manifolds and the initialization problem for some atmospheric equations. *Physica D 14*, 203–215.

Kraichnan, R. 1967. Inertial ranges in two-dimensional turbulence. *Phys. Fluids 101*, 1417–1423.

Kreiss, H. 1979. Problems with different timescales for ordinary differential equations. *SIAM J. Numer. Anal. 16*, 980–988.

Leith, C. 1980. Nonlinear normal mode initialization and quasi-geostrophic theory. *J. Atmos. Sci. 37*, 958–968.

Lorenz, E. 1980. Attractor sets and quasi-geostrophic equilibrium. *J. Atmos. Sci. 37*, 1685–1699.

Machenhauer, B. 1977. On the dynamics of gravity oscillations in a shallow water model with applications to normal mode initialization. *Beitr. Phys. Atmos. 50*, 253–271.

Sadourny, R. 1975. The dynamics of finite difference models of the shallow water equations. *J. Atmos. Sci. 32*, 680–689.

Vautard, R. and Legras, B. 1985. Invariant manifolds, quasi-geostrophy and initialization. *J. Atmos. Sci.*, in press.

Warn, T. 1986. The statistical mechanical equilibria of the shallow water equations. *Tellus 38A*, 1–11.